Recent Topics on Injection and Combustion in High Speed Flow (Keynote)

Sadatake Tomioka

Japan Aerospace eXploration Agency, Kakuda Space Center, Kakuda, Japan

Wall flush mounted injector with various orifice shape and injection conditions, were examined to enhance jet penetration and mixing in supersonic cross flow, in view of application to air-breathing accelerator vehicle. Orifice shapes with high aspect ratio were found to preferable for better penetration in the cold flow, and in the reacting flow for scramjet-mode combustion conditions. However, the effectiveness of the high aspect ratio was diminished in the dual-mode combustion conditions. Supersonic injection was applied to the high aspect ratio orifice, and further increase in penetration was observed in the cold and reactive flow for scramjet-mode combustion conditions, however, mixing enhancement due to mixing layer / pseudo-shock wave system interaction was dominant in the dual-mode combustion conditions. Difficulty in attaining ignition in the case with the high aspect ratio orifice was encountered during the combustion tests.

Nomenclature

A	: cross-sectional area
D	: injector diameter
H	: penetration height
M	: Mach number
p, P	: static pressure, total pressure
q	: jet / airflow dynamic pressure ratio
Rb	: effective radius (Ref. 10)
t, T	: static temperature, total temperature
$X, \underline{X}$	: streamwise location from injector center, onset of divergence
Y	: spanwise location from duct center
Z	: height from injector-side wall
ϕ	: equivalence ratio

Subscripts

0	: in airflow plenum
j	: fuel jet
w	: at wall

1. Introduction

Penetration / mixing enhancements of the fuel jet into / with high speed airflow are key issues to adopt ram / scramjet technologies for hypersonic cruisers and/or launch accelerators. Many injection schemes are proposed and tested for decades [e.g., Ref. 1,2].

In research efforts on a rocket based combined-cycle engine embedding rocket engine within a scramjet flow-pass [3], non-intrusive wall flush mount injectors are found to be beneficial as intrusive injectors may cause excess total pressure loss, drag and thermal load on the injection device.

Jet / airflow interactions and resulting separation in the vicinity of the orifice were to suppress the fuel jet penetration into the airflow, so that so-called wedged shape injector was proposed [4]. Further extended research on this kind of injectors has been carried out at JAXA, in collaboration with Tohoku university, Keio university, and Tokyo Institute of Technology [5-8]. In this presentation, the research activity is outlined.

2. Experimental apparatus and measurements

Mixing studies with inert gas injection into a room temperature M2.5 airflow were followed by combustion studies with hydrogen injection into a high enthalpy M2.5 airflow.

2.1. Experimental apparatus

The experiments were conducted in a blow-down type wind tunnel facility, shown in Fig. 1. Airflow with either a total temperature (T_0) of 288 K and total pressure (P_0) of 0.75 MPa ± 5%, or a total temperature (T_0) of 2000 K ± 50 K and total pressure (P_0) of 1.0 MPa ± 5%, was supplied to a Mach 2.5 rectangular nozzle with the exit cross-sectional area of 51 mm (height) by 94.3 mm (width). For the combustion tests, a vitiation heater with set-up oxygen supply was used, with oxygen mole fraction being 21.0 vol.% ± 5%, and water vapor mole fraction being approximately 26 %.

A rectangular combustor was directly connected to the nozzle. For the mixing studies, the cross-section of the combustor remained constant while its length was varied to examine the streamwise growth of the plume. For the combustion studies, the cross-section of the combustor remained constant for 507 mm from the nozzle exit, and then expanded in its height direction at an angle of 1.66 degrees for 635 mm, while the width was constant to be 94.3 mm through the combustor. The resulting exit area of the diverging section was 87.8 mm (height) by 94.3 mm (width).

In the mixing tests, the streamwise (X) coordinate was from the center of the injector orifice (defined as X = 0), and the Y and Z coordinates were in the spanwise direction from the center of the combustor and in the spanwise directions from the injector-side wall. In the combustion tests, the streamwise ($\underline{X}$) coordinate was from the onset of the diverging section (defined as $\underline{X}$ = 0). Note that the injector was mounted on one wall, so that the flow field was not symmetry in the Z direction.

2.2. Injector installation

Through this presentation, single injector orifice

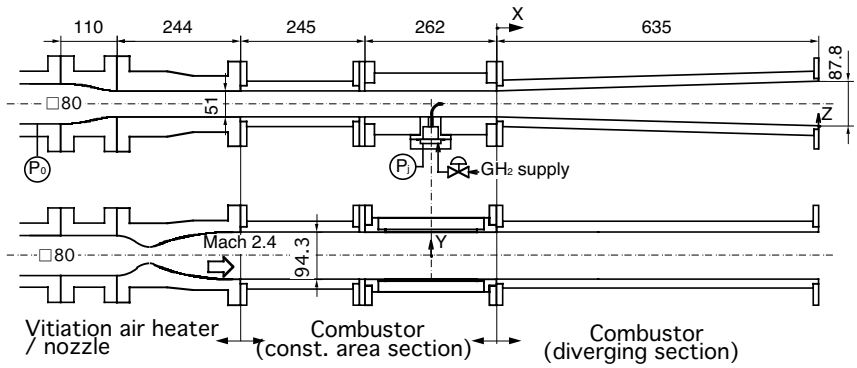

Figure 1: Schematic diagram of facility and combustor

was used for each orifice shape, which located on the centerline (Y=0 axis) of the injector-side wall (Z=0). Room temperature injectant was pressure-regulated and fed to the injectant plenum (P_j monitored).

In chapter 4.2, a 15-mm-deep, 90-mm-long 2D recess with the swept-back aft-wall at 60 degrees, was installed to attain better ignition performance. A portion of the fuel was introduced directly to the recess, if necessary for ignition promotion.

2.3. Measurements

Wall pressure (p_W) was measured with mechanical scanning-type pressure sensors. Their ranges were 0-340 kPa and 0-670 kPa with ± 0.1 % full scales uncertainties. To mitigate the run-to-run deviation of the test conditions, the measured pressure was normalized with the measured total pressure of the incoming flow (P_0).

Gas sampling was carried out at several stations for the mixing studies, and at the combustor exit (X=635 mm) for the combustion studies with water-cooled probe rakes ensuring reaction quenching during the sampling process [9]. The sampled gases were analyzed with gas chromatography with an accuracy of ±0.2 vol. % for each composition. In the combustion tests, reacted amount of hydrogen was deduced from oxygen consumption and was added to detected hydrogen to attain local fuel concentration. From the injectant volumetric concentration distributions, penetration height (h) defined as the height of the maximum concentration point from the injector-side wall was obtained. Note that the measured concentrations were time-averaged values over the sampling duration (1.4 sec.). Thus, the sampling technique only provides time- (and streamwise spatial-) averaged results.

3. High aspect ratio, sonic injectors

Sonic injection scheme with various orifice shapes was pursued for better penetration. The key feature was to reduce the airflow / jet interaction, namely the separation ahead of the jet.

3.1. Mixing studies

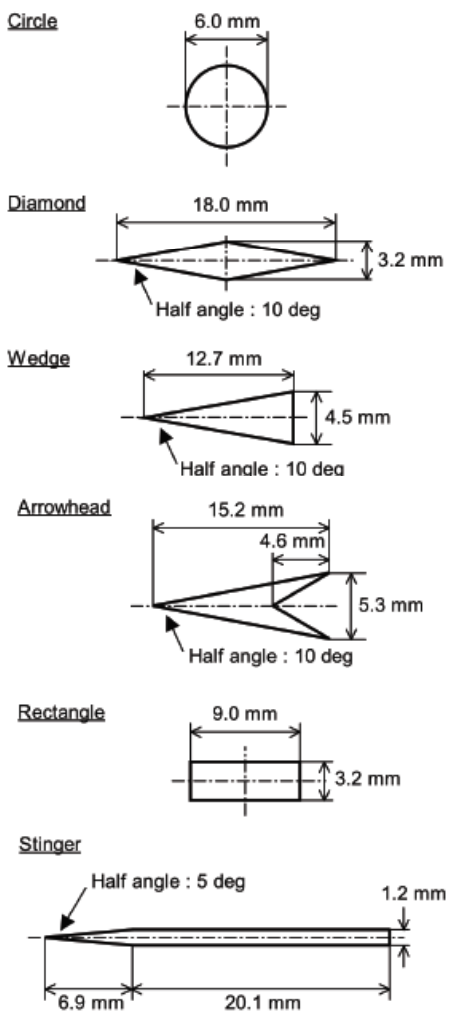

Figure 2: Injector configurations

Figure 2 shows the sonic orifice shapes used for the mixing studies. Note that all had an identical orifice area equivalent to a circular injector with 6

mm diameter (D). Thus, the injection pressure, and thus the dynamic pressure ratio, was identical for an injectant mass flow rate, while only small deviations due to difference in discharge coefficients was left.

Figure 3 shows the injectant concentration (in volume %) distributions with several orifice shapes at X = 131 mm at the dynamic pressure ratio of about unity. The wedge shaped injector to reduce the jet / airflow interaction showed better penetration than the ordinal circular injector, and penetration was increased by reducing the wedge angle. Penetration further increased with reduced orifice width at fixed wedge shape angle (i.e., by using the stinger shaped orifice). Thus, the orifice aspect ratio was expected to be the dominant factor for penetration.

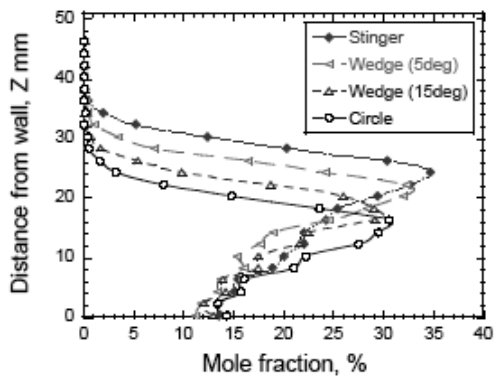

Figure 3: Injectant concentration distributions on X-Z plane at X=131 mm.

Figure 4 shows the relation between the orifice's aspect ratio and the penetration height. A larger aspect ratio resulted in a larger penetration height. Numerical simulations showed that injection through the high aspect ratio injector resulted in lower surface pressure in the vicinity of the orifice, so that the aspect ratio dominated the jet / airflow interaction.

Figure 5 shows the variation of the penetration height (at X = 131 mm) against the jet to airflow dynamic pressure ratio, in the cases with the stinger-shaped and circular injectors. In the case with the circular injector, the penetration height was almost proportional to the square root of the dynamic pressure ratio, as reported in many studies. In comparison to the circular injector, the stinger-shaped injector showed quite higher penetration at lower dynamic pressure ratio (q < 2), but lower penetration at higher dynamic pressure (q > 3). At higher q (and thus higher Pj), the jet became under-expanded condition, and selectively expanded to the spanwise direction (so-called axis-switching) to become an obstacle against the airflow, and resulting intensive jet / airflow interaction reduced the penetration.

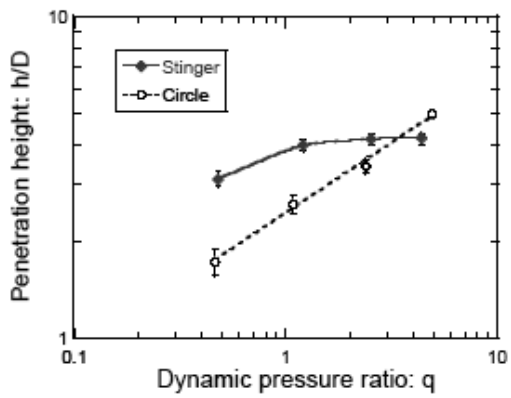

Figure 5: Variation of penetration height at X=131 mm against dynamic pressure ratio.

3.2. Combustion studies

The stinger-shaped injector was applied to the combustion studies, and its characteristics were compared to those of the circular injector.

Figure 6 compares the wall pressure distributions with the stinger-shaped and circular injectors at various fuel equivalence ratios. The stinger-shaped

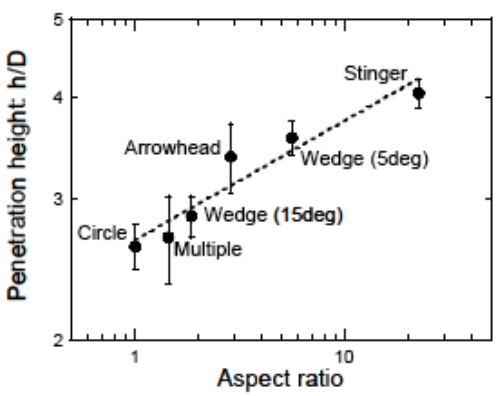

Figure 4: Relation between penetration height at X=131 mm and aspect ratio.

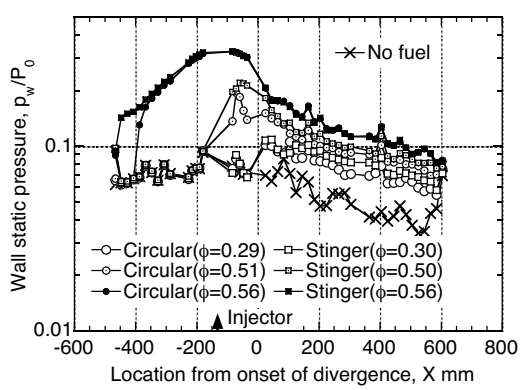

Figure 6: Wall pressure distributions with stinger-shaped and circular injectors

injection resulted in higher pressure-rise in the scramjet-mode combustion regime (pressure-rise only at downstream to the injector) due to better penetration / mixing characteristics than that with the circular injection as will be shown in Fig. 7, until the pressure-rise was anchored at the injector location ($\phi \sim 0.5$). At this fuel flow rate, the stinger-shaped injection caused more intensive pressure-rise in the vicinity of the orifice, though the circular injection tends to cause more intensive jet / airflow interaction favorable for ignition and flame-holding. Cause of this discrepancy was not yet revealed. In the dual-mode combustion regime, the pressure level was almost identical to that with the circular injector.

Figure 7 shows the local equivalence distributions on X-Z plane at the combustor exit, in the scramjet-mode ($\phi = 0.3$) and when the pressure-rise was anchored at the injector location ($\phi = 0.5$). Injection through the stinger-shaped injector resulted in higher penetration than that through the circular injector in the scramjet-mode, while it lower by the transition to the dual-mode. Increase in the injection pressure increased the dynamic pressure ratio, so that the stinger-shaped injector became less effective as predicted in Fig. 5. So-called matched pressure injection condition (jet static pressure ~ back-pressure to the jet) is optimal in these high-aspect-ratio injection schemes.

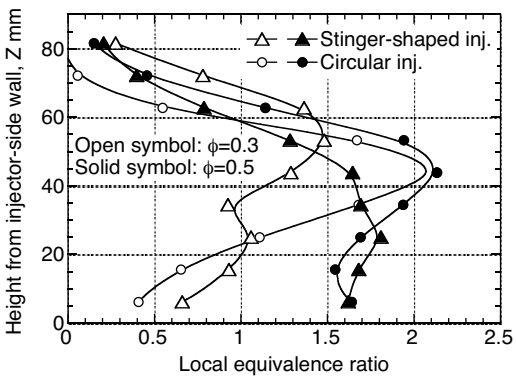

Figure 7: Fuel distribution at exit of combustor with stinger-shaped and circular injectors.

4. Supersonic injections

The low (or matched) pressure injection beneficial for penetration for the high-aspect-ratio injector, can not be applied to the accelerator vehicle with varying airflow condition as an increase in the back-pressure to the jet may violate the choking condition at the orifice. Thus, supersonic injection with high Pj and low jet static pressure was applied to a high-aspect-ratio injector (diamond-shaped one due to easier fabrication).

4.1. Mixing studies

Several matched-pressure injection schemes were applied, and their penetration / mixing characteristics were compared to those with the sonic injection scheme. All injection schemes had diamond-shaped orifices with identical half-angle of 10 degrees, but with different throat area and expansion ratio. Figure 8 shows the orifice shapes. At design flow rate, the large sonic injector was in matched-pressure condition, i.e, the jet static pressure matched with the ambient back-pressure. The small injector with 15% throat orifice area was in under-expanded condition with sonic injection, however, the Mj=2.4 small injector was in the matched-pressure condition. The Mj=1.9 medium injector with 30% throat orifice area was also in the matched-pressure condition.

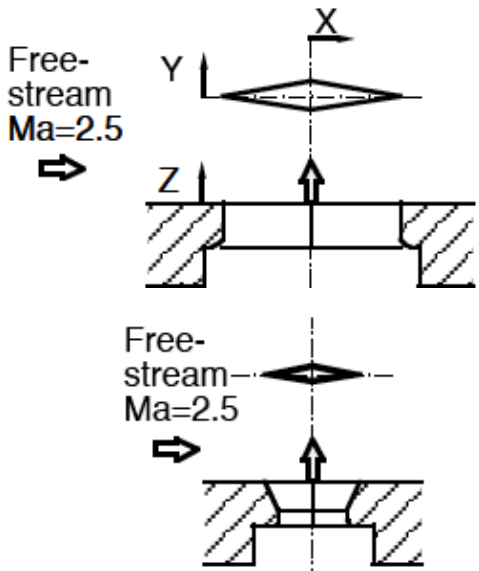

Figure 8: Diamond-shaped orifices. (upper: sonic orifice, lower; supersonic orifice)

Figure 9 summarized penetration height growth with various schemes including circular sonic injection. Note that both the streamwise distance and penetration height were normalized with

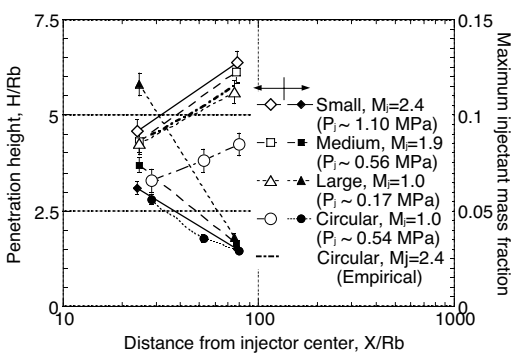

Figure 9: Penetration growth with several injection configurations.

effective radius [10] to take slight difference in the flow rate into account. All matched-pressure injection through diamond-shaped orifices showed better penetration than the sonic under-expanded injection through the circular orifice. Though not shown in the figure, the under-expanded sonic injection through the diamond-shaped orifice resulted in almost identical penetration to that through the circular orifice at this high q of 2.4. A higher jet Mach number resulted in slightly higher penetration.

Figure 10 shows the penetration characteristics at various injection conditions in the cases with the small supersonic diamond-shaped injector and the circular injector. In the case with the circular injector, a higher injection pressure resulted in a higher penetration as previous studies shown. However, in the case with the supersonic, diamond-shaped injector, a lower injection pressure resulted in a higher penetration. Over-expansion of the jet squeezed the jet in the spanwise direction to make the jet thinner, resulted in better penetration.

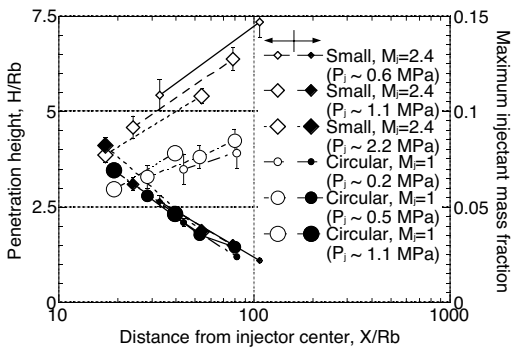

Figure 10: Penetration growth with various injection conditions.

4.2. Combustion studies

The supersonic injection through the high-aspect ratio, diamond-shaped injector was found to be beneficial for dual-mode operation with increasing airflow pressure due to occurrence of the pseudo-shock system, as the over-expanded condition was found to be favorable for better penetration. Thus, this injection scheme was applied to the combustion studies, and its characteristics were compared to those of the circular injector.

Figure 11a compares the wall pressure distributions with the supersonic diamond-shaped injector and the sonic circular injector. At $\phi = 0.3$, combustion was in scramjet-mode, i.e., pressure-rise due to combustion observed at downstream portion to the injector. The onset of pressure-rise was around the onset of the diverging section in both injection cases. In the far field, pressure-rise was more intensive with the supersonic diamond-shaped injector due to better penetration as will be shown in

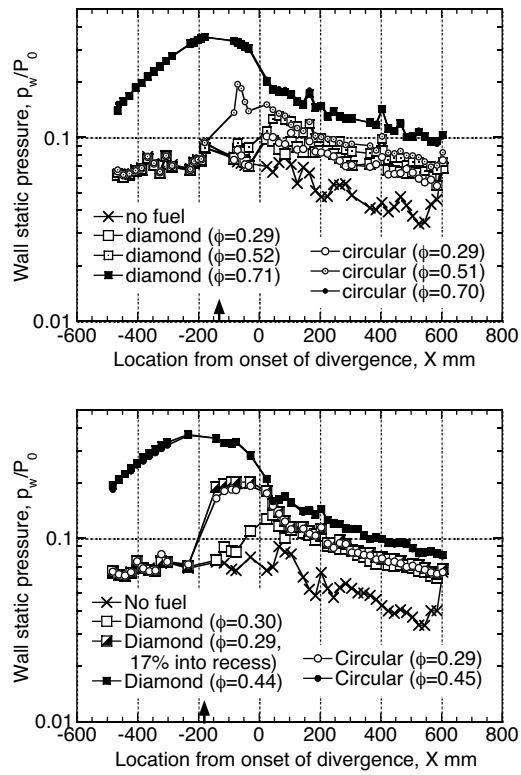

Figure 11: Wall pressure distributions with diamond-shaped and circular injectors a) without (upper) and b) with (lower) recess.

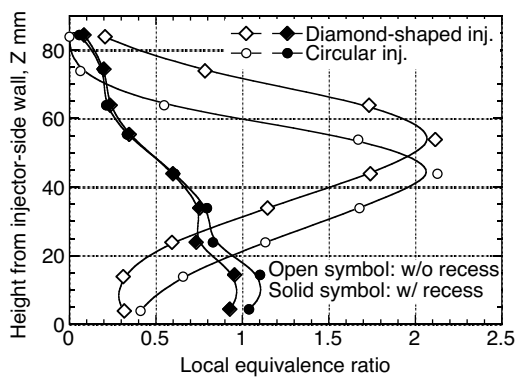

Figure 12: Fuel distribution at exit of combustor with diamond-shaped and circular injectors.

Fig. 12. With increase in the fuel flow rate, pressure-rise occurred in the vicinity of the orifice with the sonic circular injector, resulted in a higher pressure-level within the whole combustor than that with the supersonic diamond-shaped injector. Thus, occurrence of the pressure-rise in the vicinity of the injector (i.e., interaction between the jet and pseudo-

shock wave system) in the near field, had sizable effects on the mixing process. One should note that the supersonic injection through the diamond-shaped orifice showed less ignition ability than the latter. With further fuel flow rate, so-called dual-mode combustion occurred in both injector cases, and the resulting pressure distributions were almost identical.

A recess was installed to enhance ignition and a portion (17%) of the fuel was fed into the recess directly, for the case with the supersonic diamond-shaped injector. Figure 11b shows the wall pressure distributions. The pressure-level in the near field was now almost identical between these two injector cases, pressure-rise being anchored in the vicinity of the injector at $\phi = 0.3$. The resulting pressure level was almost identical, slightly higher with the diamond-shaped injector. With increase in the fuel flow rate, transition to the dual-mode occurred in both injector cases, and the pressure level became almost identical. Note that the transition occurred at a lower fuel flow rate even in the case with the circular injector.

Figure 12 shows the local equivalence distributions on X-Z plane at the combustor exit, in the scramjet-mode ($\phi = 0.3$, without recess) and when the pressure-rise was anchored at the injector location ($\phi = 0.3$, with the recess). In the scramjet-mode combustion, the supersonic injection through the diamond-shaped orifice shows better penetration than the sonic injection through the circular injector. It was also found that combustion efficiency was better in the former injection scheme within the shear layer at the airflow side. Once the flame was anchored in the vicinity of the orifice, there were drastic changes in the distributions, the fuel jet core was no longer visible and mixing was enhanced due to shear flow / pseudo-shock wave system interaction. The thinner mixture than in the scramjet-mode case implied that the spanwise diffusion of the jet was also intensive. In this condition, the fuel diffusion was better with the diamond-shaped orifice in the vicinity of the injection-side wall.

5. Conclusions

Experimental and numerical studies were carried out on the wall flush mount injection scheme for better penetration and mixing within ram / scramjet / RBCC engines. The joint research activities by JAXA, Tohoku university, Keio university and Tokyo Institute of Technology were herein summarized.

References

1) G. B. Northam, I. Greenberg, C. S. Byington, and D. P. Capriotti, 'Evaluation of Parallel Injector Configurations for Mach 2 Combustion,' *J. Propulsion and Power*, Vol. 8, No. 2, pp. 491-499, 1992.
2) M. R. Gruber, J. M. Donbar, C. D. Carter, and K. –Y. Hsu, 'Mixing and Combustion Studies Using Cavity-Based Flameholders in Supersonic Flow,' *J. Propulsion and Power*, Vol. 20, No. 5, pp.769-778, 2004.
3) T. Kanda and K. Kudo, 'Conceptual Study of a Combined-Cycle Engine for an Aerospace Plane,' *J. Propulsion and Power*, Vol. 19, No. 5, pp.859-867, 2003.
4) M. J. Barber, J. A. Schetz, and L. A. Roe, 'Perpendicular, Sonic Helium Injection through a Wedge-Shaped Orifice into Supersonic Flow,' *J. Propulsion and Power*, Vol. 13, No. 2, pp. 257-263, 1997..
5) Hirano, K. Matsuo, A., Kouchi, T., Tomioka, S., Izumikawa, M., 'New Injector Geometry for Penetration Enhancement of Perpendicular Jet into Supersonic Flow,' AIAA paper 2007-5028, Jul. 2007.
6) T. Kouchi, K. Hirano, A. Matsuo, K. Kobayashi, S. Tomioka, and M. Izumikawa, 'Combustion Performance of Supersonic Combustor with Stinger-Shaped Fuel Injector,' AIAA Paper 2008-4503, Jul. 2008.
7) S. Tomioka, M. Izumikawa, T. Kouchi, G. Masuya, K. Hirano, and A. Matsuo, 'Matched Pressure Injections into a Supersonic Crossflow through Diamond-Shaped Orifices,' *J. Propulsion and Power*, Vol. 24, No. 3, pp. 471-478, 2008.
8) S. Tomioka, T. Kohchi, R. Masumoto, M. Izumikawa and A. Matsuo, 'Supersonic Combustion with Supersonic Injection through Diamond-shaped Orifices,' AIAA paper 2009-5229, Aug. 2009
9) T. Mitani, M. Takahashi, S. Tomioka, T. Hiraiwa, and K. Tani, 'Analysis and Application of Gas Sampling to Scramjet Engine Testing,' *J. Propulsion and Power*, Vol. 15, No. 4, pp. 572-577, 1999.
10) J. A. Schetz, 'Interaction Shock Shape for Transverse Injection in Supersonic Flow,' *Journal of Spacecrafts and Rockets*, Vol. 7, No. 2, pp.143-149, 1970.